Polymer 51 (2010) 5952–5959

Contents lists available at ScienceDirect

Polymer

journal homepage: www.elsevier.com/locate/polymer

Nanoparticle formulation of poly(ε-caprolactone-*co*-lactide)-D-α-tocopheryl polyethylene glycol 1000 succinate random copolymer for cervical cancer treatment

Yuandong Ma [a,b], Laiqiang Huang [a,b], Cunxian Song [c], Xiaowei Zeng [d], Gan Liu [d], Lin Mei [a,b,*]

[a] School of Life Sciences, Tsinghua University, Beijing 100084, PR China
[b] The Shenzhen Key Lab of Gene and Antibody Therapy, Center for Biotech and Bio-Medicine and Division of Life Sciences, Graduate School at Shenzhen, Tsinghua University, Shenzhen, Guangdong Province, 518055, PR China
[c] Institute of Biomedical Engineering, Peking Union Medical College & Chinese Academy of Medical Sciences, The Tianjin Key Laboratory of Biomaterial Research, Tianjin 300192, PR China
[d] Key Laboratory of Functional Polymer Materials, Ministry of Education, Institute of Polymer Chemistry, Nankai University, Tianjin 300071, PR China

ARTICLE INFO

Article history:
Received 6 March 2010
Received in revised form
20 September 2010
Accepted 13 October 2010
Available online 21 October 2010

Keywords:
PCL-PLA-TPGS
Random copolymer
Nanoparticles

ABSTRACT

Cervical cancer remains a critical problem that is second only to breast cancer affecting women worldwide. The objective of this study was to develop formulation of docetaxel-loaded biodegradable poly (ε-caprolactone-*co*-lactide)-D-α-tocopheryl polyethylene glycol 1000 succinate (PCL-PLA-TPGS) nanoparticles for cervical cancer chemotherapy. A novel random copolymer, PCL-PLA-TPGS, was synthesized from ε-caprolactone, lactide and D-*a*-tocopheryl polyethylene glycol 1000 succinate (TPGS) by ring-opening polymerization. The obtained polymers were characterized by ^{1}H NMR, FTIR, GPC and TGA. The docetaxel-loaded PCL-PLA-TPGS nanoparticles were prepared by a modified solvent extraction/evaporation technique and characterized in terms of size and size distribution, morphology, surface charge and physical state of encapsulated docetaxel. Cellular uptake and *in vitro* cytotoxicity of nanoparticle formulations were done in comparison with commercial formulation Taxotere® to investigate the efficacy of PCL-PLA-TPGS nanoparticles. In vitro cellular uptakes of such nanoparticles were investigated with CLSM, demonstrating the coumarin 6-loaded PCL-PLA-TPGS nanoparticles could be internalized by Hela cells. *In vitro* cancer cell viability experiment showed that judged by IC_{50}, the PCL-PLA-TPGS nanoparticle formulation was found to be more effective in cell number reduction than the Taxotere® after 48 h ($p < 0.05$), 72 h ($p < 0.05$) treatment. In conclusion, the PCL-PLA-TPGS copolymer could be acted as a novel and promising biologically active polymeric matrix material for nanoparticle formulation in cervical cancer treatment.

1. Introduction

Cervical cancer remains a critical problem that is second only to breast cancer affecting women worldwide [1]. However, in clinics, the current approaches for cancer treatment are still limited to surgical resection, irradiation, and chemotherapy. These are highly invasive or nonspecific, and often accompanied by side effects and toxicity to normal cells. The promises of nanotechnology in cancer research lie in the potential to solve these problems [2]. The pathophysiological condition and anatomical changes of diseased tissues offers many advantages for the delivery of nanoparticles [3]. The physiology of diseased tissues may be altered in a variety of physiological conditions and can be exploited for passively targeting of drugs [4]. The increased vascular permeability coupled with an impaired lymphatic drainage in tumors allows an enhanced permeability and retention effect of the nanoparticles in the tumors [3,5]. In addition, the important technological advantages of nanoparticles used as drug carriers are high stability, high drug loading capacity, protection of incorporated labile drugs from degradation, controlled release, excellent tolerability and feasibility of variable routes of administration like parenteral, oral, dermal, ocular, pulmonary, and rectal [6]. Nanoparticles could also reduce the multi-drug resistance that characterizes many anticancer drugs by a mechanism of internalization of the drug [7], reducing its efflux from cells mediated by the P-glycoprotein [8]. Therefore,

* Corresponding author. The Shenzhen Key Lab of Gene and Antibody Therapy, Center for Biotech and Bio-Medicine and Division of Life Sciences, Graduate School at Shenzhen, Tsinghua University, L401, Tsinghua Campus, Xili University Town, Shenzhen Guangdong Province 518055, PR China. Tel.: +86 755 26036381; fax: +86 755 26036052.
E-mail address: mei.lin@sz.tsinghua.edu.cn (L. Mei).

0032-3861/$ – see front matter © 2010 Elsevier Ltd. All rights reserved.
doi:10.1016/j.polymer.2010.10.029

nanotechnology is considered to be an emerging, disruptive technology that will have a profound impact in all sectors of industry and across-the-board applications in cancer research.

During the past decade, polymeric microspheres, polymeric nanoparticles, polymer micelles, and hydrogel-type materials have all been shown to be effective in enhancing drug targeting specificity, lowering systemic drug toxicity, improving treatment absorption rates, and providing protection for pharmaceuticals against biochemical degradation. In addition, several other experimental drug delivery systems show exciting signs of promise, including those composed of biodegradable polymers, dendrimers (so-called star polymers), electroactive polymers, and modified C-60 fullerenes (also known as "buckyballs"). Early research into biodegradable systems focused on naturally occurring polymers (collagen, cellulose, etc.) but has recently moved into the area of chemical synthesis. Examples of such polymers include polyanhydrides, polyesters, polyacrylic acids, poly(methyl methacrylates), and polyurethanes. In recent years, increasing attention has been paid to biodegradable aliphatic polyesters such as poly (ε-caprolactone) (PCL) and polylactide (PLA) for applications in the fields of surgery, nanoparticle-based drug delivery system and tissue engineering [9–11]. Stereo copolymerization between lactide enantiomers leads to PLA with variable stereoregularity and is a useful approach to adjust degradability, as well as mechanical and physical properties [12]. In the past decade, PCL has attracted considerable interest because of its outstanding permeability, thermal property and biocompatibility [11,13]. Random co-polymerization is known to provide new copolymers with properties intermediate to those of the corresponding homopolymers [14,15]. This is a valuable method to fine-tune properties to the desired parameters. D-α-tocopheryl polyethylene glycol 1000 succinate (TPGS) is a water-soluble derivative of natural vitamin E. The chemical structure of TPGS is similar to that of other amphiphiles, comprising hydrophilic polar head group and lipophilic alkyl tail. Its bulky structure and large surface area make it become an excellent solubilizer, emulsifier, bioavailability enhancer of hydrophobic drugs. TPGS-emulsified nanoparticles have been shown higher drug encapsulation and cellular uptake, longer half life and higher therapeutic effects of the formulated drug than those emulsified by poly(vinyl alcohol) (PVA), a widely used emulsifier in nanoparticle technology [16]. Moreover, Vitamin E TPGS could improve drug permeability through cell membranes by inhibiting P-glycoprotein, and thus enhance absorption of drugs and reduce P-glycoprotein mediated multi-drug resistance in tumor cells [17–19]. It has been found that TPGS could effectively inhibit the growth of human lung carcinoma cells from *in vitro* cell culture and implanted in nude mice [20]. The superior anticancer efficacy of TPGS is associated with its increasing ability to induce apoptosis and not due to its increased cell uptake into cells [20–22]. Synergistic effects could be obtained by the use of combinations of vitamin E isomers or derivatives in the presence of other anticancer agents [21]. We were thus inspired to synthesize PCL-PLA-TPGS random copolymer for nanoparticle formulation of small molecule drug chemotherapy. Docetaxel was used as a model anticancer drug due to its excellent therapeutic effects against a wide spectrum of cancers and its great commercial success as the best seller among all the antineoplastic agents.

2. Materials and methods

2.1. Materials

D,L-lactide (3,6-dimethyl-1,4-dioxane-2,5-dione, $C_6H_8O_4$) was purchased from Aldrich, Milwaukee, USA. ε-caprolactone (CL) was obtained from Acros Organics (Geel, Belgium). D-α-tocopheryl polyethylene glycol 1000 succinate (TPGS, $C_{33}O_5H_{54}$ $(CH_2CH_2O)_{23}$) was from Sigma (St. Louis, MO, USA). Poly(ε-caprolactone) (PCL) (MW 42000 Da), stannous octoate ($Sn(OOCC_7H_{15})_2$) and 3-(4,5-dimethylthiazol-2-yl)-2,5-diphenyltetrazolium bromide (MTT) were also supplied from Sigma (St. Louis, MO, USA). Docetaxel of purity 99.8% was purchased from Shanghai Jinhe Bio-Technology Co. Ltd (Shanghai, China). Acetonitrile and methanol were purchased from EM Science (ChromAR, HPLC grade, Mallinckrodt Baker, USA). All other chemicals used were of the highest quality commercially available. Ultrahigh pure water produced by Boon Environmental Tech. Industry Co., Ltd (Tianjin, China) was used throughout all experiments. Human cervix carcinoma HeLa cells were provided by American Type Culture Collection (ATCC, Rockville, MD).

2.2. Synthesis of PCL-PLA-TPGS random copolymer

PCL-PLA-TPGS random copolymers were synthesized from ε-caprolactone, lactide and TPGS in the presence of stannous octoate as a catalyst via ring opening polymerization. In short, preweighted amounts of ε-caprolactone, lactide, TPGS and one drop of stannous octoate were added in a flask. The mixture was heated to 145 °C and allowed to react for approximately 16 h. Synthesis was carried out under an oxygen- and moisture-free environment. The product was dissolved in DCM and then precipitated in excess cold methanol to remove unreacted monomers and TPGS. The final product was collected by filtration and dried under vacuum.

2.3. Characterization of PCL-PLA-TPGS random copolymer

FTIR spectrophotometer (Thermo Nicolet, Madison, WI, USA) was used to investigate the molecular structure of PCL-PLA-TPGS random copolymer. Briefly, the samples for FTIR analysis were prepared by grinding 99% KBr with 1% copolymer and then pressing the mixture into a transparent tablet. The TPGS content and number-averaged molecular weight of the copolymer was determined by ^1H NMR in $CDCl_3$ at 300 Hz (Bruker ACF300). The weight-averaged molecular weight and molecular weight distribution were determined by gel permeation chromatography (GPC). Thermogravimetric analysis (TGA, TGA 2050 thermogravimetric analyzer, USA) was carried out to investigate the thermal properties of the copolymers. During the TGA analysis, about 5–15 mg of the copolymer sample was heated from 0 °C to 600 °C at a rate of 10 °C/min. The weight loss pattern in the copolymer thermogram can be related to the composition of the random copolymers.

2.4. Formulation of PCL-PLA-TPGS nanoparticles

Docetaxel-loaded PCL-PLA-TPGS nanoparticles were fabricated by a modified solvent extraction/evaporation technique as described previously [10]. Briefly, a given amount of docetaxel and 100 mg PCL-PLA-TPGS random copolymer were fully dissolved in 8 ml dichloromethane (DCM). The formed solution was poured into 120 ml of 0.03% (w/v) TPGS solution under gentle stirring. The mixture was sonicated for 2 min at 25 W output to form O/W emulsion. The emulsion was then evaporated overnight under reduced pressure to remove the organic solvent. The particle suspension was centrifuged at 22,000 rpm for 20 min and then washed three times to remove the emulsifier and unencapsulated drug. The resulted particles were resuspended in 10 ml water and freeze-dried for two days. In addition, the fluorescent coumarin-6 loaded nanoparticles were prepared in the same way except 0.1% (w/v) coumarin-6 was encapsulated instead of docetaxel.

2.5. Characterization of PCL-PLA-TPGS nanoparticles

2.5.1. Particle size and size distribution analysis

Size and size distribution of the docetaxel-loaded PCL-PLA-TPGS nanoparticles were determined by Dynamic Light Scattering (Zetasizer Nano ZS90, Malvern Instruments LTD., Malvern, UK). The particles (about 2 mg) were suspended in deionized water before measurement.

2.5.2. Surface morphology

The particle morphologies were examined by a field emission scanning electron microscopy (FESEM) using a JEOL JSM-6700F system operated at a 5.0 kV accelerating voltage. To prepare samples for FESEM, the particles were fixed on the stub by a double-sided sticky tape and then coated with platinum layer by JFC-1300 automatic fine platinum coater (JEOL, Tokyo, Japan) for 40 s.

2.5.3. Zeta potential

The particles (about 2 mg) were suspended in deionized water before measurement. Zeta potential of the nanoparticles was measured by Laser Doppler Anemometry (LDA; Zetasizer Nano ZS90, Malvern Instruments LTD., Malvern, UK).

2.5.4. Drug loading and encapsulation efficiency

Drug loading content and encapsulation efficiency (EE) of the nanoparticles was determined by HPLC (LC 1200, Agilent Technologies, Santa Clara, CA) according to previously published methods [10]. Briefly, 5 mg nanoparticles were dissolved in 1 ml DCM under vigorous vortexing. This solution was transferred to 5 ml of mobile phase consisting of deionized water and acetonitrile (50:50, v/v). A nitrogen stream was introduced to evaporate the DCM for about 15 min, and then a clear solution was obtained for HPLC analysis. A reverse-phase Inertsil® C-18 column (150 mm × 4.6 mm, pore size 5 mm, GL science Inc, Tokyo, Japan) was used. The flow rate of mobile phase was 1 ml/min. The column effluent was detected at 227 nm with a UV/VIS detector. The drug encapsulation efficiency was defined as the ratio between the amount of docetaxel encapsulated in the nanoparticles and that added in the process.

2.5.5. Differential scanning calorimetry

The physical status of docetaxel inside the nanoparticles was investigated by differential scanning calorimetry (DSC 822e, Mettler Toledo, Greifensee, Switzerland). The samples were purged with dry nitrogen at a flow rate of 20 ml/min. The temperature was raised at 10 °C/min.

2.5.6. In vitro drug release

Briefly, 15 mg docetaxel-loaded nanoparticles were dispersed in 5 ml release medium (phosphate buffer solution of pH 7.4 containing 0.1% w/v Tween 80) to form a suspension. Tween 80 was

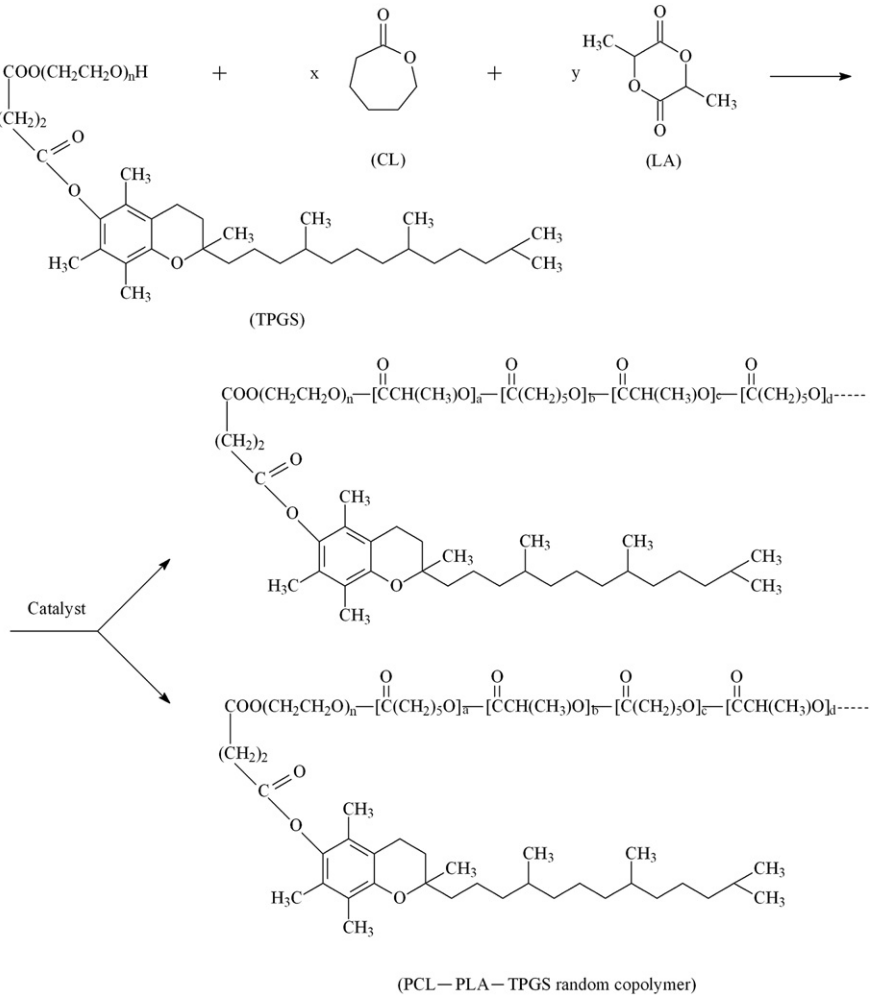

Fig. 1. Schematic description of the synthesis of PCL-PLA-TPGS random copolymer.

used to increase the solubility of docetaxel in the buffer solution and avoid the binding of docetaxel to the tube wall. The suspension was transferred into a Regenerated Cellulose Dialysis Membrane (Spectra/Por 6, MWCO = 1000, Spectrum, Houston, TX, USA). Then, the closed bag was put into a centrifuge tube and immersed in 15 ml release medium. The tube was put in an orbital water bath shaking at 120 rpm at 37.0 °C. 10 ml of solutions were periodically removed for analysis and replaced with fresh medium. The collected samples were extracted with 2 ml DCM and reconstituted in 5 ml mobile phase. A nitrogen stream was introduced to evaporate the DCM. The analysis procedure was the same as for the measurement of encapsulation efficiency. The PCL-PLA-TPGS (Sample D) and PCL nanoaprticles (Sample H) with 0.03% TPGS as surfactant and 10% drug loading were used for *in vitro* drug release studies.

2.6. Cellular uptake of nanoparticles

HeLa cells were cultivated in the chambered cover glass system with 5% CO_2 in the Dulbecco's modified Eagle medium (DMEM) at 37 °C. After the cells were incubated with 250 μg/ml coumarin-6 loaded nanoparticles (Sample G) at 37 °C for 4 h, the cells were rinsed with cold PBS for three times and then fixed by methanol for 20 min. The nuclei of the cells were stained by 4′,6-diamidino-2-phenylindole dihydrochloride (DAPI, Fluka, Buche, Switzerland) for about 5 min. The cells were washed twice again with PBS. In order to visualize the cells, the chambers were mounted onto the confocal laser scanning microscope (CLSM, Olympus Fluoview FV-1000, Olympus Optical. Co., Ltd., Tokyo, Japan) with imaging software. The images of the cells were determined with differential interference contrast (DIC) channel, and the images of coumarin-6 loaded nanoparticles and the nuclei of the cells stained by DAPI were recorded with following channels: blue channel (DAPI) with excitation at 340 nm and green channel (coumarin-6) with excitation at 488 nm [23].

2.7. In vitro cell viability

HeLa cells were seeded in 96-well plates at the density of 5000 viable cells per well and incubated 24 h to allow cell attachment. The cells were incubated with docetaxel-loaded PCL-PLA-TPGS nanoparticle suspension and commercial Taxotere® at 0.25, 2.5, 12.5 and 25 μg/ml equivalent docetaxel concentrations and drug-free PCL-PLA-TPGS nanoparticle suspension with the same amount of nanoparticles for 24, 48 and 72 h, respectively. At determined time, the formulations were replaced with DMEM containing MTT (5 mg/ml) and cells were then incubated for additional 4 h. MTT was aspirated off and DMSO was added to dissolve the formazan crystals. Absorbance was measured at 570 nm using a microplate reader (Bio-Rad Model 680, UK). Untreated cells were taken as control with 100% viability and cells without addition of MTT were used as blank to calibrate the spectrophotometer to zero absorbance. IC50, the drug concentration at which inhibition of 50% cell growth was observed, in comparison with that of the control sample, was calculated by curve fitting of the cell viability data.

2.8. Statistical methodology

The results are expressed as mean ± SD. The significance of differences was assessed using Student's t test, and was termed significance when $p < 0.05$.

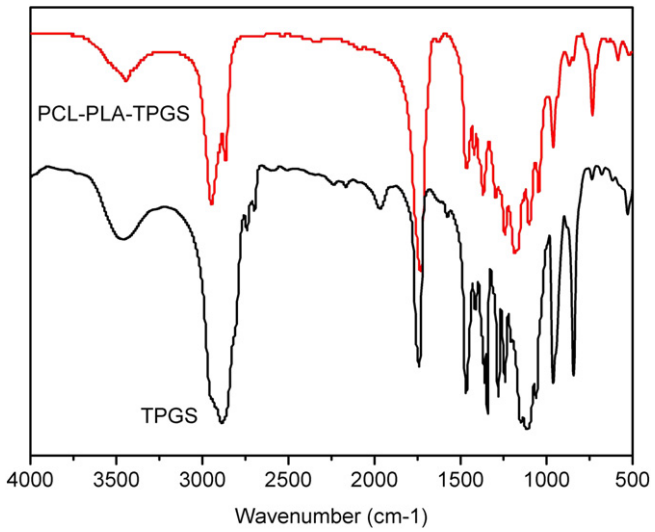

Fig. 2. FTIR spectra of TPGS and PCL-PLA-TPGS random copolymer.

3. Results and discussions

3.1. Synthesis and characterization of PCL-PLA-TPGS random copolymer

The PCL-PLA-TPGS copolymer was synthesized via the ring-opening co-polymerization of ε-caprolactone (CL), lactide and TPGS by using the stannous octoate as catalyst. The mechanism of synthesis, which is similar to that in synthesis of the PLA-PCL-PEG-

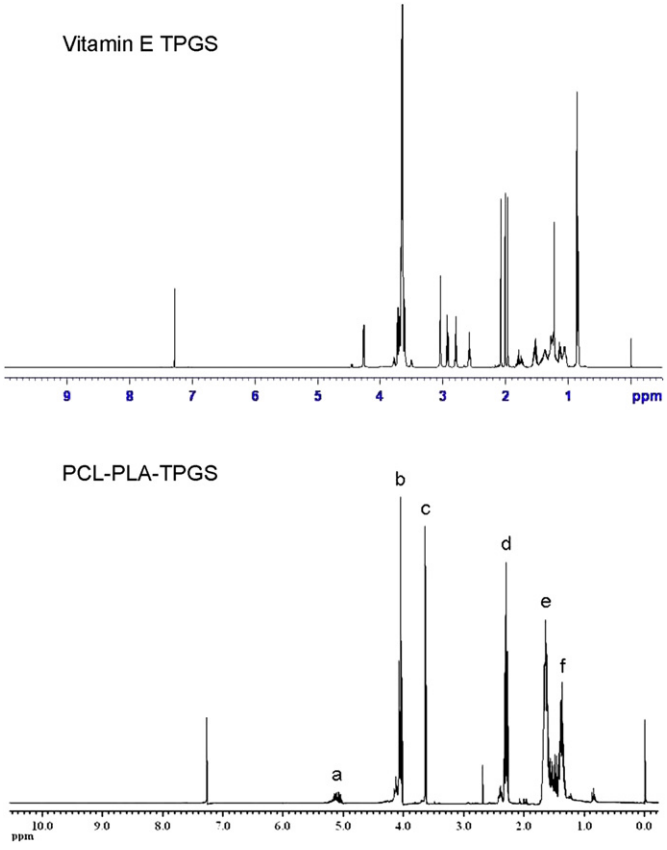

Fig. 3. Typical ^{1}H NMR spectra of TPGS and PCL-PLA-TPGS random copolymer.

PCL-PLA copolymer [24] and PLGA–TPGS copolymer [16], is schematically described in Fig. 1.

Fig. 2 shows the FTIR spectra of the PCL-PLA-TPGS copolymer and TPGS. The carbonyl band of TPGS appears at 1739 cm^{-1}. For the synthesized copolymer, the carbonyl band was shifted to 1731 cm^{-1}, which was different with the carbonyl bands of PLA at 1745 cm^{-1} and of PCL at 1725–1726 cm^{-1} [25,26]. In the PCL-PLA-TPGS spectrum, the bands in the range 2867–2947 cm^{-1} are assigned to $-CH_2$ stretching band of PCL, the CH_2 stretching band of PLA at 2945 cm^{-1} and that of TPGS at 2880 cm^{-1} was not been observed because of overlapping with that of PCL-PLA-TPGS. The absorption band at 3400–3650 cm^{-1} is attributed to the terminal hydroxyl group and that at 1045–1295 cm^{-1} is due to the C–O stretching [27]. Of those, the band at 1241 cm^{-1} is assigned to asymmetric COC stretching [28]. The band at 1295 cm^{-1} has been used in the literature to investigate the crystallinity change in PCL [29].

The structure of the synthesized PCL-PLA-TPGS copolymer was detected by ^1H NMR in $CDCl_3$. Fig. 3 shows a typical ^1H NMR spectroscopy of the PCL-PLA-TPGS copolymer. The signals at 5.2 and 1.69 ppm (Fig. 3 peak a and peak e) were assigned to the CH protons and methyl protons $-CH_3$ of PLA segment, respectively [16]. The peak at 3.65 ppm (Fig. 3 peak c) was assigned to the $-CH_2$ protons of PEO part of TPGS [23]. The lower peaks in the aliphatic region belong to various moieties of vitamin E tails [30–34]. The peaks at 4.06(peak b), 2.31 (peak d), 1.60–1.70 (peak e) and 1.35–1.43 (peak f) were assigned to $-OCH_2$, $-COCH_2$, $-CH_2$ (4H) and $-CH_2$ (2H) segment of PCL, respectively [24]. The molecular weight of the PCL-PLA-TPGS was calculated by using the ratio between the peak areas at 4.06 (peak area: 9.64), 5.2 (peak area: 1.23) and 3.65 (peak area: 3.00). The number-averaged molecular weight of the PCL-PLA-TPGS random copolymer was determined to be 33,229. The feeding ratio of ε-caprolactone, lactide and TPGS molecular mass was 75%, 15% and 10%, respectively. However, the ratio of ε-caprolactone, lactide and TPGS molecular mass which were integrated into the PCL-PLA-TPGS copolymers is 87.18%, 8.17% and 4.64%.

In GPC analysis, we confirmed that the PCL-PLA-TPGS copolymer was synthesized by the ring-opening polymerization. The product was not a physical mixture of TPGS with lactide and ε-caprolactone. Fig. 4 shows that the peak for TPGS appeared at 28.23 min. Instead, the peak of the copolymer shifted to 17.51 min. The polydispersity of the copolymer molecular weight was narrow, around 1.32. The number-averaged molecular weight calculated from the GPC chromatograph was 35,209. It seemed that the molecular weight detected from GPC and NMR can confirm each other.

TGA was performed on the synthesized copolymers in order to investigate their thermal properties. Fig. 5 shows the typical thermal degradation profiles for TPGS monomer and PCL-PLA-TPGS copolymer. It was observed that the thermal degradation profiles of PCL-PLA-TPGS copolymer showed two main regions of weight loss, which were different from a single mass loss for the TPGS monomer. Each turning point marked the combustion of a new component in the copolymers. The 200–380 °C and 380–450 °C combustion zones were attributed to PLA-PCL and TPGS part of copolymers, respectively. The results further confirmed the successful synthesis of PCL-PLA-TPGS copolymer. Huang et al. also found that PLA-PCL-PEG-PCL-PLA copolymers showed a biphasic thermal degradation profile [24].

3.2. Characterization of PCL-PLA-TPGS nanoparticles

The size and size distribution of the PCL-PLA-TPGS nanoparticles prepared in this research are shown in Table 1. Owing to a self emulsifying function of the TPGS component in the copolymer, the drug-loaded nanoparticles can be prepared with or without addition of TPGS as surfactant in the nanoparticle fabrication process. The particle size was found around 160 nm with narrow size distribution of less than 0.2 polydispersity for samples without addition of TPGS. It can be seen from Table 1 that addition of TPGS in the process as emulsifier slightly increased the particle size. The particle size was found around 200 nm with size distribution of less than 0.4 polydispersity for samples with addition of TPGS. It is reasonable that the coating effects of TPGS on the particle surface and extra TPGS on the particle surface may cause aggregation of the formed nanoparticles and increase the size of nanoparticles. There were also evidences showing the TPGS amphipathic surfactants align themselves at the oil–water interface to promote the stability of the particles by lowering the surface energy and thus resist coalescence and flocculation of the particles [16].

It can be seen that the PCL-PLA-TPGS nanoparticles prepared without addition of emulsifier can result in a lower drug EE than those prepared with emulsifier. For samples without addition of TPGS, the drug encapsulation efficiency was found to increase from 21.00% for 10% drug loading to 69.89% for 2.5% drug loading. For

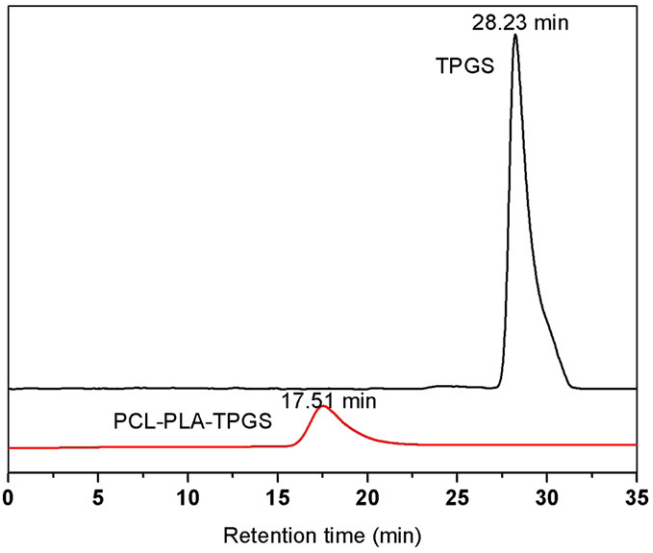

Fig. 4. Typical GPC chromatograms of TPGS and PCL-PLA-TPGS random copolymer.

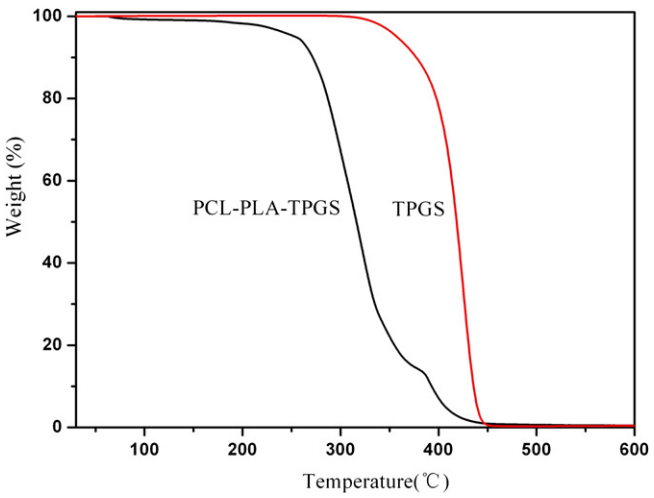

Fig. 5. Thermogravimetric profiles of TPGS and PCL-PLA-TPGS random copolymer.

Table 1
Characterization of nanoparticle formulations.

Sample No.	Polymer	Theoretical drug loading	Surfactant	Size (nm)	PDI	ZP (mV)	EE (%)
A	PCL-PLA-TPGS	2.5%	No	148.82 ± 5.64	0.114 ± 0.03	−34.85 ± 0.55	69.89 ± 3.25
B	PCL-PLA-TPGS	5%	No	163.51 ± 6.38	0.117 ± 0.04	−32.11 ± 0.45	54.42 ± 2.94
C	PCL-PLA-TPGS	10%	No	182.33 ± 4.56	0.202 ± 0.02	−35.49 ± 0.69	21.00 ± 5.73
D	PCL-PLA-TPGS	10%	0.03% TPGS	195.82 ± 5.24	0.371 ± 0.03	−28.17 ± 0.15	97.87 ± 2.11
E	PCL-PLA-TPGS	10%	0.06% TPGS	251.50 ± 6.46	0.379 ± 0.02	−23.16 ± 0.47	81.57 ± 3.14
F	PCL-PLA-TPGS	0	0.03% TPGS	184.51 ± 2.77	0.213 ± 0.12	−36.48 ± 0.26	0
G	PCL-PLA-TPGS	*	0.03% TPGS	201.36 ± 4.61	0.271 ± 0.17	−38.29 ± 0.70	Not shown
H	PCL	10%	0.03% TPGS	252.42 ± 6.48	0.309 ± 0.03	−16.56 ± 0.14	89.12 ± 3.42

* = Coumarin 6, PDI = Polydispersity index, ZP = Zeta potential, EE = Encapsulation efficiency, $n = 3$.

samples with the addition of TPGS, however, the drug encapsulation efficiency increased significantly to 100% for 10% drug loading when 0.03% TPGS was added as emulsifier and to 81.56% when 0.06% TPGS was added. It has been shown that the surfactant used in the fabrication process and the drug loading level are important factors to influence the particle size and size distribution and the drug encapsulation efficiency in the release kinetics, cellular uptake and thus the therapeutic effects of the drug-loaded nanoparticles [35,36]. An appropriate amount of TPGS for PLGA nanoparticle formulation of paclitaxel would be 0.03% w/w. Too little emulsifier would not be enough to cover the interface, and too much emulsifier would cause particle aggregation.

Formulation stability is of key importance and zeta potential measurements are instrumental in developing stable dispersions. High absolute value of the zeta potential suggests high surface charge of the nanoparticles, which leads to strong repellent interactions among the nanoparticles in dispersion and thus high stability. As shown in Table 1, zeta potential of PCL-PLA-TPGS nanoparticles is −28.17 mV. Compared with PCL nanoparticles, whose zeta potential is around −16.56 mV, a great increase in the absolute value of zeta potential for PCL-PLA-TPGS nanoparticles could be observed, indicating higher dispersion stability. The negative surface charge of PCL-PLA-TPGS nanoparticles may be attributed to the presence of ionized carboxyl groups of PLA and PCL segments on the nanoparticles surface.

Surface morphology of the drug-loaded PCL-PLA-TPGS nanoparticles was examined by FESEM. Fig. 6 shows the FESEM images of the docetaxel-loaded PCL-PLA-TPGS nanoparticles. The particles seemed to have a spherical shape and a smooth surface within the FESEM resolution level. The FESEM images further confirmed the particle size detected from the Dynamic Light Scattering.

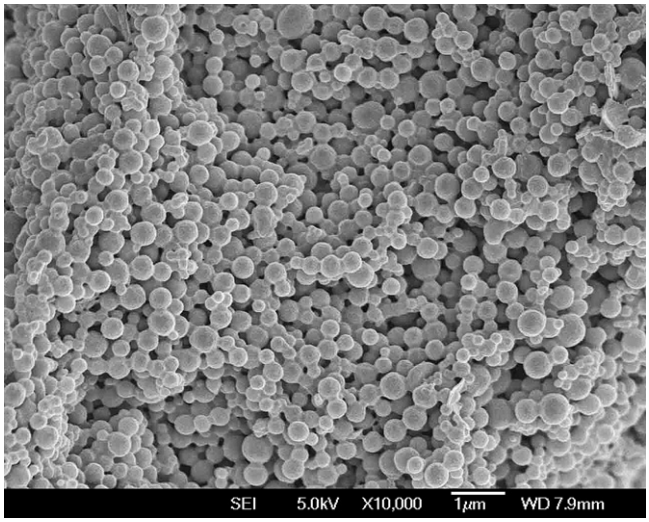

Fig. 6. FESEM images of docetaxel-loaded PCL-PLA-TPGS nanoparticles with 0.03% TPGS as emulsifier and 10% drug loading.

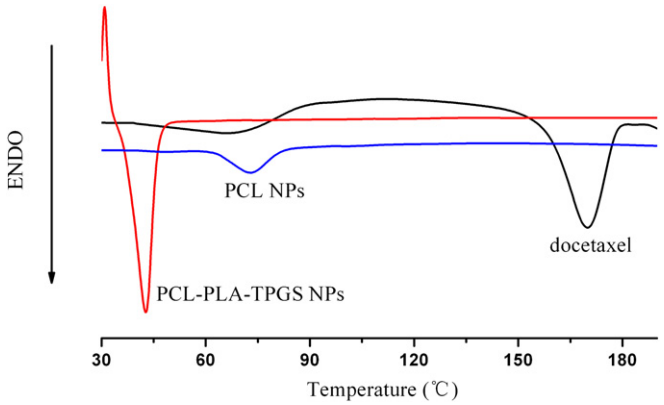

Fig. 7. DSC thermograms of pure docetaxel, docetaxel-loaded PCL-PLA-TPGS nanoparticles (Sample D) and docetaxel-loaded PCL nanoparticles (Sample H).

Differential Scanning Calorimetry (DSC) studies were performed to investigate the physical state of docetaxel in the nanoparticles, because this aspect could influence the *in vitro* and *in vivo* drug release from the nanoparticle formulation. Fig. 7 shows the DSC thermograms of pure docetaxel, docetaxel-loaded PCL-PLA-TPGS nanoparticles and docetaxel-loaded PCL nanoparticles. The melting

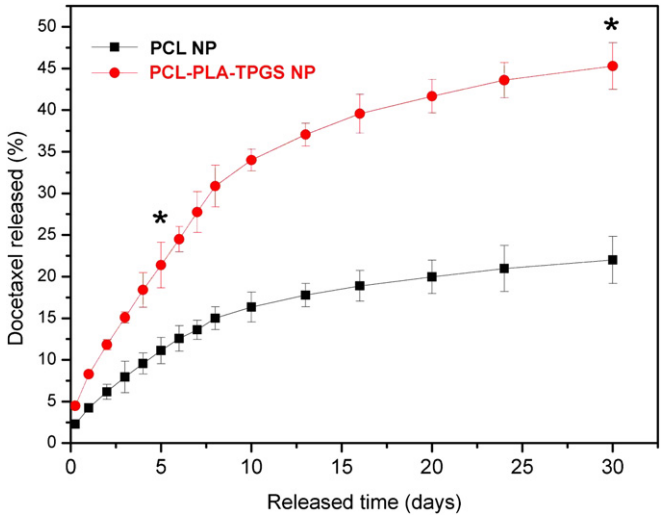

Fig. 8. The *in vitro* release profile of docetaxel-loaded PCL (Sample H) and PCL-PLA-TPGS nanoparticles (Sample D). Compared with PCL nanoparticles, drug release from PCL-PLA-TPGS nanoparticles was significantly faster in the first 5 days and after 30 days (*$p < 0.05$).

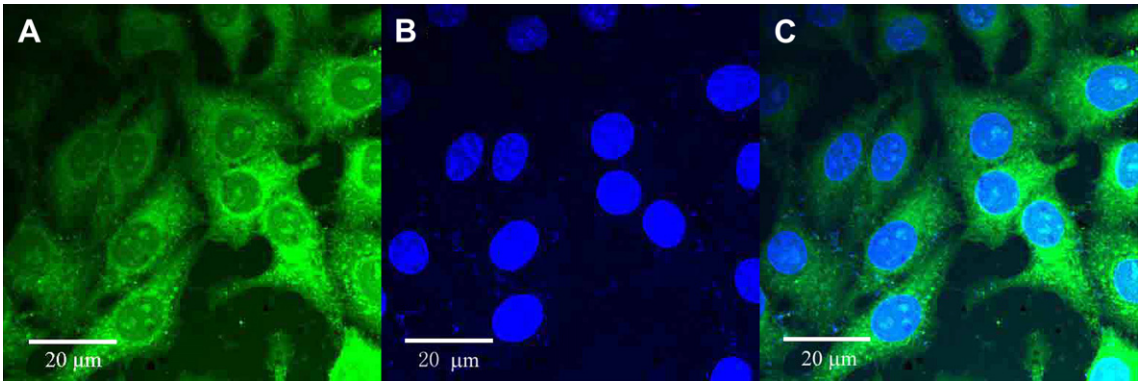

Fig. 9. Confocal laser scanning microscopy (CLSM) images of HeLa cells after 4 h incubation with coumarin 6-loaded PCL-PLA-TPGS nanoparticles (Sample G) at 37.0 °C. The cells were stained by DAPI (blue) and the coumarin 6-loaded nanoparticles are green. The cellular uptake was visualized by overlaying images obtained by EGFP filter and DAPI filter: left image from EGFP channel (A); center image from DAPI channel (B); right image from combined EGFP channel and DAPI channel (C). (For interpretation of the references to colour in this figure legend, the reader is referred to the web version of this article).

endothermic peak of pure docetaxel appeared at 173 °C. However, no melting peak was detected for nanoparticle formulations. It can thus be concluded that docetaxel in the nanoparticle formulation was in an amorphous or disordered crystalline phase or in the solid solution state.

The *in vitro* drug release profiles of the docetaxel-loaded nanoparticles in the first 28 days are shown in Fig. 8. The drug release from the PCL-PLA-TPGS nanoparticles (Sample D) was found to be 21.38% and 45.29% of the encapsulated drug in the first 5 days and after 30 days, respectively, which was much faster than the docetaxel-loaded PCL nanoparticles (Sample H), which is only 11.12% and 22.01%, respectively, in the same periods. The faster drug release of the PCL-PLA-TPGS nanoparticles may be attributed to the lower molecular weight and the higher hydrophilicity of PCL-PLA-TPGS copolymer in comparison with the PCL nanoparticles. It causes the copolymer to swell and to degrade faster, thus promoting the drug release from the nanoparticles. In comparison with the traditional PCL nanoparticles which were found to release the drug too slowly to meet the therapeutic needs, this is another advantage of the PCL-PLA-TPGS nanoparticles when applied to cancer therapy.

3.3. Cellular uptake of coumarin 6-loaded PCL-PLA-TPGS nanoparticles

Fig. 9 shows confocal laser scanning microscopy (CLSM) images of the HeLa cancer cells after 24 h incubation with the coumarin-6 loaded PCL-PLA-TPGS nanoparticle (Sample G) suspension in the Dulbecco's modified Eagle medium (DMEM) at 250 μg/ml nanoparticle concentration. The images were obtained from (A) the EGFP (green) channel; (B) the DAPI (blue) channel; (C) the overlay of the two channels. It can be observed from Fig. 9 that the coumarin 6-loaded PCL-PLA-TPGS nanoparticles (green) were closely located around the nuclei (blue, stained by DAPI), indicating the nanoparticles had been internalized into the cells. In this research, TPGS may enhance the cellular uptake of the nanoparticles by inhibiting P-glycoprotein [16–19].

3.4. In vitro cell viability of nanoparticles

The *in vitro* cytotoxic activity of drug-free nanoparticles (Sample F) and docetaxel-loaded nanoparticles (Sample D) was evaluated by the MTT assay using the HeLa cell line. The range of concentrations of docetaxel (0.25–25 μg/ml) was selected because it corresponds to plasma levels of the drug achievable in humans [37]. It can be concluded from Fig. 10 that in general (1) there was no obvious cytotoxic activity for the drug-free PCL-PLA-TPGS nanoparticles at various concentration from 0.25 μg/ml to 25 μg/ml, (2) the docetaxel-loaded PCL-PLA-TPGS nanoparticles achieved significantly higher cytotoxicity against HeLa cells than commercial Taxotere® after 48 h and 72 h incubation and (3) the cellular viability decreased with the incubation period for both Taxotere® and nanoformulations. The HeLa cell viability after 24 h incubation at the 12.5 μg/ml drug concentration was 78.35 ± 4.01% for Taxotere® and 86.22 ± 2.46% for docetaxel-loaded PCL-PLA-TPGS nanoparticles. However, compared with commercial Taxotere®, the cell

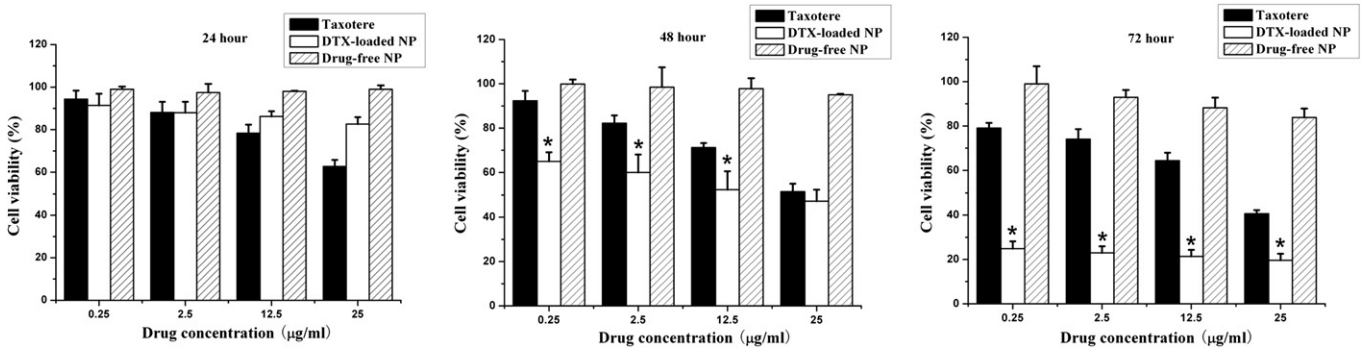

Fig. 10. Viability of HeLa cells cultured with docetaxel-loaded PCL-PLA-TPGS nanoparticles (Sample D) in comparison with that of Taxotere® at the same docetaxel dose and drug-free PCL-PLA-TPGS nanoparticles (Sample F) with the same amount of nanoparticles ($n = 3$). Compared with Taxotere®, significant reduction in cell number for PCL-PLA-TPGS nanoparticles could be observed ($^*p < 0.05$).

Table 2
IC50 of HeLa cells after 24, 48 and 72 h of incubation with docetaxel formulated in the Taxotere® and PCL-PLA-TPGS nanoparticle formulation (Sample D).

Incubation time (h)	IC_{50} (μg/ml)	
	PCL-PLA-TPGS NPs (Sample D)	Taxotere®
24	687.0	127.7
48	19.3	47.9
72	4.6	28.1

number of HeLa cells was reduced by 65.4% ($p < 0.05$, $n = 5$) and 120.65% ($p < 0.05$, $n = 5$) for docetaxel-loaded PCL-PLA-TPGS nanoparticle formulation after 48 h and 72 h incubation at the 12.5 μg/ml drug concentration. In addition, there were statistically significant differences between Taxotere® formulation and docetaxel-loaded PCL-PLA-TPGS nanoparticle formulation for the HeLa cell viability after 72 h incubation at all concentrations (Fig. 10, $p < 0.05$, $n = 5$). The results also indicated time- and concentration-dependence of cell number reduction against HeLa cells for PCL-PLA-TPGS nanoparticle formulation.

The *in vitro* therapeutic effects of a formulation can be quantitatively evaluated by its IC_{50}, which is defined as the drug concentration at which 50% of the cells in culture have been killed in a designated time period. Table 2 gives IC50 of HeLa cells after 24, 48, 72 h incubation with docetaxel formulated in the Taxotere® and PCL-PLA-TPGS nanoparticles. The results showed that the IC_{50} value for HeLa cells was 687.0 μg/ml for nanoparticle formulation, which is significantly higher than that of Taxotere® after 24 h incubation. However, the IC_{50} value for HeLa cells was decreased from 47.9 to 28.1 μg/ml for Taxotere® to 19.3 and 4.6 μg/ml for nanoparticle formulation after 48 and 72 h incubation. As time goes by, the nanoparticle formulation showed better and better *in vitro* therapeutic effects for HeLa cells than commercial Taxotere®. This is because the accumulative drug release was only 4.6%, 8.3% and 12.2% for PCL-PLA-TPGS nanoparticles after 24, 48 and 72 h (Fig. 8), respectively, and the release started from 0% while the Taxotere® immediately became 100% available for the HeLa cells in culture. Furthermore, the degradation of PCL-PLA-TPGS copolymers may release the TPGS components, which have synergistic anticancer activity in the presence of anticancer agent [21–23], thus resulting in higher and higher cytotoxicity (Fig. 10).

4. Conclusion

For the first time, the PCL-PLA-TPGS random copolymers were successfully synthesized in this research for nanoparticle formulation of small molecular anticancer drugs with docetaxel as a model drug. The docetaxel-loaded PCL-PLA-TPGS nanoparticles were prepared by a modified solvent extraction/evaporation technique. The drug encapsulation efficiency of PCL-PLA-TPGS nanoparticle formulation was improved greatly with the addition of 0.03% TPGS. The size of such nanoparticles was found to be around 200 nm. The docetaxel-loaded PCL-PLA-TPGS nanoparticles could achieve much faster drug release in comparison with PCL nanoparticles. *In vitro* cellular uptakes of such nanoparticles were investigated with CLSM, demonstrating the coumarin 6-loaded PCL-PLA-TPGS nanoparticles could be internalized by human cervix carcinoma cells (HeLa). The results also showed advantages of PCL-PLA-TPGS nanoparticle formulation over commercial Taxotere® in terms of cytotoxicity against HeLa cells. In conclusion, the PCL-PLA-TPGS copolymer could be acted as a novel and promising biologically active polymeric matrix material for nanoparticle formulation in cervical cancer treatment.

Acknowledgements

The authors are grateful for financial support from the National Natural Science Foundation of China (No 30900291), China Postdoctoral Science Foundation (No. 20090450030), Shenzhen Bureau of Science, Technology & Information (No. JC200903180531A) and Shenzhen Nanshan Science and Technology Program (KJ02S0210900000109). The author owes an especial debt of gratitude to Prof. Feng Si-shen for his advice and assistance.

References

[1] Parkin DM, Pisani P, Ferlay J. Cancer J Clin 1999;49:33.
[2] Kim KY. Nanomedicine: NBM 2007;3:103.
[3] Sahoo SK, Parveen S, Panda JJ. Nanomedicine: NBM 2007;3:20.
[4] Vasir JK, Labhasetwar V. Technol Cancer Res Treat 2005;4:363.
[5] Maeda H, Wu J, Sawa T, Matsumura Y, Hori K. J Control Release 2000;65:271.
[6] Bawarski WE, Chidlowsky E, Bharali DJ, Mousa SA. Nanomedicine: NBM 2008;4:273.
[7] Davda J, Labhasetwar V. Int J Pharm 2002;233:51.
[8] Brigger I, Dubernet C, Couvreur P. Adv Drug Deliv Rev 2002;54:631.
[9] Chang KY, Lee YD. Acta Biomater 2009;5:1075.
[10] Zhang Y, Tang L, Sun L, Bao J, Song C, Huang L, et al. Acta Biomater 2010;6(6):2045.
[11] Vert M. J Mater Sci Mater Med 2009;20:437.
[12] Li S, Garreau H, Vert M. J Mater Sci Mater Med 1990;1:123.
[13] Sun H, Mei L, Song C, Cui X, Wang P. Biomaterials 2006;27:1735.
[14] Pitt CG. Poly(ε-caprolactone) and its copolymers. In: Chasin M, Langer R, editors. Biodegradable polymers as drug delivery systems. New York: Marcel Dekker; 1990. p. 71–120.
[15] Li X, Wu Q, Chen Z, Gong X, Lin X. Polymer 2008;49:4769.
[16] Ma Y, Zheng Y, Liu K, Tian G, Tian Y, Xu L, et al. Nanoscale Res Lett 2010;5(7):1161–9.
[17] Fischer JR, Harkin KR, Freeman LC. Vet Tech Res Appl Vet Med 2002;3:465.
[18] Dintaman JM, Silverman JA. Pharm Res 1999;16:1550.
[19] Yu L, Bridgers A, Polli J, Vicker A, Long S, Roy A, et al. Pharm Res 1999;16:1812.
[20] Youk HJ, Lee E, Choi MK, Lee YJ, Chung JH, Kim SH, et al. J Control Release 2005;107:43.
[21] Constantinou C, Papas A, Constantinou AI. Int J Cancer 2008;123:739.
[22] Neuzil J, Tomasetti M, Zhao Y, Dong LF, Birringer M, Wang XF, et al. Mol Pharmacol 2007;71:1185.
[23] Feng SS, Mei L, Anitha P, Gan CW, Zhou W. Biomaterials 2009;30:3297.
[24] Huang MH, Suming L, Coudane J, Vert M. Macrom Chem Phy 2003;204:1994.
[25] Pamula E, Blazewicza M, Paluszkiewiczb Cz, Dobrzynski P. J Mol Struct 2001;596:69.
[26] Lin WJ, Lee HG. J Control Release 2003;89:179.
[27] Liu K, Kiran E. Polymer 2008;49:1555.
[28] Li SH, Woo EM. Colloid Polym Sci 2008;286:253.
[29] Elzein T, Nasser-Eddine M, Delaite C, Bistac S, Dumas P. J Colloid Interface Sci 2004;273:381.
[30] Mosmann T. J Immunol Methods 1983;65:55.
[31] Neuzil J. Br J Cancer 2003;89:1822.
[32] Birringer M, EyTina JH, Salvatore BA, Neuzil J. Br J Cancer 2003;88:1948.
[33] Momot KI, Kuchel PW, Chapman BE, Deo P, Whittaker D. Langmuir 2003;19:2088.
[34] Schroder H, Netscher T. Magn Reson Chem 2001;39:701.
[35] Win KY, Feng SS. Biomaterials 2005;26:2713.
[36] Mei L, Zhang Y, Zheng Y, Tian G, Song C, Yang D, et al. Nanoscale Res Lett 2009;4:1530–9.
[37] Raymond E, Hanauske A, Faivre S, Izbicka E, Clark G, Rowinsky EK. Anticancer Drugs 1997;8:379.